

**Energy transfer in collisions of metal clusters with multiply charged ions**J. Daligault,<sup>1,2</sup> F. Chandezon,<sup>1,\*</sup> C. Guet,<sup>1,3</sup> B. A. Huber,<sup>1,4</sup> and S. Tomita<sup>1,5</sup><sup>1</sup>*Département de Recherche Fondamentale sur la Matière Condensée, CEA-Grenoble, 17, rue des Martyrs, F-38054 Grenoble Cedex 9, France*<sup>2</sup>*Los Alamos National Laboratory, Theoretical Division, MS-K 717, Los Alamos, New Mexico 87545*<sup>3</sup>*Département de Physique Théorique et Appliquée, CEA-DAM-Ile de France, Boîte Postale 12, F-91680 Bruyères-le-Chatel, France*<sup>4</sup>*CIRIL-GANIL, Rue Claude Bloch, Boîte Postale 5133, F-14070 Caen Cedex 05, France*<sup>5</sup>*Institute of Physics and Astronomy, University of Aarhus, DK-8000 Aarhus C, Denmark*

(Received 22 April 2002; published 27 September 2002)

Collisions between low-energy multiply charged ions and neutral metal clusters are an efficient method to investigate charge instabilities in finite systems. We study here the appearance size  $n_{app}(q)$  of multiply charged sodium clusters  $\text{Na}_n^{q+}$  with  $q \leq 10$ , i.e., the smallest size of observation for  $q$ -fold charged clusters and its dependence on the collision parameters. The experimental results are compared with the energy transferred to the cluster during the collision, calculated with the semiclassical Vlasov equation within the jellium approximation. Experimental and theoretical data show similar trends with the collision parameters and evidence the importance of dynamical effects. These results guide further investigations for studying low excited multiply charged finite systems.

DOI: 10.1103/PhysRevA.66.033205

PACS number(s): 36.40.Qv, 31.15.Gy, 34.50.Gb

**I. INTRODUCTION**

Collisions between highly charged low-energy ions (velocities below 1 a.u.) and atomic clusters or fullerenes have recently emerged as a new field since pioneering experiments with fullerenes and metal clusters [1–3]. The motivations in this field of collisions physics are manifold. On one hand, fullerenes or clusters represent for projectile ions a target intermediate between atoms and bulk surfaces. Clusters retain the finite size of atoms while possessing a large number of low bound electrons compared to the projectile charge, similar in that sense to bulk surfaces [1]. They in fact exhibit characteristics of both systems, depending on the collision impact parameter [2–4]. On another hand, collisions of highly charged low-energy ions with clusters are efficient ways to form low excited multiply charged clusters and to study the onset of charge instabilities in finite systems. In particular, for high projectile charges (typically above 10), the excitation energy transferred to the cluster in peripheral collisions can be quite low, which allows to disentangle genuine charge instabilities from thermal instabilities [5–7].

This latter method was recently applied to metallic sodium clusters [8,9]. In these experiments, the observable is the appearance size  $n_{app}(q)$ , i.e., the size below which clusters  $\text{Na}_n^{q+}$  are unstable on the experimental time scale and disappear from the spectra. Based on the theory of Lord Rayleigh for classical charged liquid conducting droplets, the appearance size at  $T=0$  K should equate the critical size  $n_{crit}(q)$ , also called the Rayleigh limit [10]. For small charges and sizes, there are deviations from the classical behavior that arise from finite-size effects either in the ionic structure or the electronic structure, the latter being dominant for simple metal clusters [11]. The balance between the Coulombic disruptive forces and the surface tension can also be

quantified by the dimensionless fissility parameter  $X = n_{crit}(q)/n$  which equates 1 at the Rayleigh limit. For sodium clusters, of interest in this paper,  $n_{crit}(q) \approx 2.5q^2$  and  $X \approx 2.5q^2/n$ . The experimental appearance sizes of sodium clusters ionized with low-energy highly charged projectile ions  $A^{z+}$  decrease when increasing  $z$  and converge towards an asymptotic limit slightly above the Rayleigh limit corresponding to a fissility  $X \approx 0.85$  [9]. This tendency was interpreted as the result of the decreasing internal energy transferred to the cluster during the collision with the ion. The departure from the Rayleigh limit was attributed to the initial cluster temperature, about 100 K.

In this paper which is an extension of our previous work [9], we compare  $n_{app}(q)$  to the excitation energy calculated with a semiclassical theory based on the Vlasov equation within the jellium approximation for the cluster description [5,12]. We study their dependence on the collision parameters: projectile charge  $z$  and velocity  $v$ , collision impact parameter  $b$ , and cluster size  $n$ . The appearance size  $n_{app}(q)$  is shown to be an indicator of the excitation energy transferred to the cluster in a peripheral collision between a projectile ion and a neutral cluster. The comparison between these two quantities shows a nontrivial dependence of the appearance size or excitation energy due to a balance between the transferred excitation energy and the internal degrees of freedom of the cluster. The calculated trends allow us to interpret experimental measurements and to guide further investigations.

The paper is organized as follows. The experiment is presented in Sec. II. In Sec. III the theoretical method is described. We discuss and compare the experimental appearance size and the theoretical transferred excitation energy in Sec. IV and their dependence on the collisions parameters. Finally, the conclusion follows in Sec. V. Unless specified otherwise, atomic units (a.u.) are used ( $e = m = \hbar = 1$ ) throughout the paper.

\*Email address: fchandezon@cea.fr

## II. EXPERIMENT

Details on the experimental apparatus can be found elsewhere [13]. In brief, neutral sodium clusters are generated in a gas aggregation source cooled with liquid nitrogen and using helium as the buffer gas. The resulting clusters are expected to be thermalized at approximately 100 K. A beam of neutral sodium clusters is formed and after passing through differential pumping stages it enters the interaction region of a high resolution reflectron time-of-flight mass spectrometer (RTOFMS) where it crosses perpendicularly a pulsed beam of ions  $A^{z+}$  with a pulse width around 10  $\mu$ s. The ion beam is provided by the Accélérateur d'Ions Multi-chargés (AIM) facility at CEA-Grenoble (now moved to GANIL accelerator in Caen). We used for these experiments ion charges  $z$  from 1 to 28 with a kinetic energy of 20 keV/charge at which the accelerator performances are optimal. Depending on the nature of the projectile ion, this corresponds to velocities around 0.5 a.u.. Alternatively the ion beam can be replaced by a laser beam (266 nm) in order to measure the primary cluster size distribution. After the ion pulse has left the interaction region (18 cm long), an electric field is switched on to extract the ionized clusters perpendicularly to the ion and neutral cluster beams. The onset provides the “start” of the RTOFMS. The orientation of the interaction region can be varied over several degrees to compensate for the neutral clusters velocity and focus the ions onto the detector. The clusters ions  $\text{Na}_n^{q+}$  then pass freely in a field-free drift zone (2 m), are reflected by a two-field reflector (50 cm), drift again in a second field-free region (1.8 m), and finally hit a microchannel plate detector. We used two cascaded rectangular microchannel plates ( $90 \times 25 \text{ mm}^2$ ) with their long axis oriented along the neutral cluster beam direction. Together with the variable orientation of the interaction region of the RTOFMS, this allows us to compensate for the initial cluster thermal velocity and to optimize the RTOFMS transmission in the size region of interest. Finally, the cluster ions arrival time on the detector is registered by an acquisition system working in an event-by-event acquisition mode, which yields a time-of-flight spectrum when integrating over all events. In the usual experimental conditions, the cluster total flight time is  $T(\text{Na}_n^{q+}) = T_0 \sqrt{n/q}$  with  $T_0 \approx 23 \mu$ s, i.e., in the 100- $\mu$ s range. A typical spectrum obtained with  $\text{Ar}^{8+}$  projectile ions ( $E = 160 \text{ keV}$ ,  $v = 0.4 \text{ a.u.}$ ) and calibrated in cluster size-over-charge ratio  $n/q$  is displayed in Fig. 1.

The mass resolution of the RTOFMS is currently  $m/\delta m_{1/2} \approx 10\,000$  ( $\delta m_{1/2}$  is the full width at half maximum of a peak) in the  $n/q$  range of interest and reaches 14 000 in optimal conditions. This allows us to identify peaks of ten-fold charged clusters [9]. The appearance size  $n_{\text{app}}(q)$  is extracted from the mass spectra by identifying the peaks corresponding to the charge  $q$  which do not overlap with peaks of lower charges. The size where the signal disappears in the background is identified as the appearance size  $n_{\text{app}}(q)$ . This is illustrated in Fig. 2 for sevenfold charged clusters  $\text{Na}_n^{7+}$  using  $\text{Xe}^{20+}$  ( $E = 400 \text{ keV}$ ,  $v = 0.35 \text{ a.u.}$ ) as projectile ions. In this case,  $n_{\text{app}}(q=7) = 186 \pm 5$  corresponding to  $X = 0.659 \pm 0.018$ .

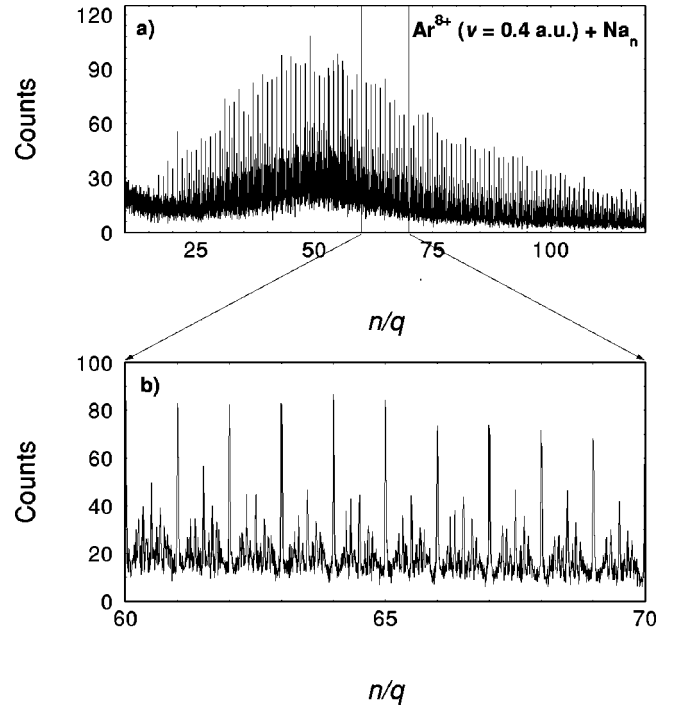


FIG. 1. (a) Time-of-flight mass spectrum of multiply charged sodium clusters  $\text{Na}_n^{q+}$  following the interaction of neutral clusters  $\text{Na}_n$  with  $\text{Ar}^{8+}$  (kinetic energy  $E = 160 \text{ keV}$ ,  $v = 0.4 \text{ a.u.}$ ) projectiles. The x axis is calibrated with the cluster size-over-charge ratio  $n/q$ . (b) Enlargement of the same spectrum. The peaks situated between the main peaks at integer values of  $n/q$  correspond to multiply charged clusters  $\text{Na}_n^{q+}$ .

## III. THEORY

Although purely classical approaches, such as the dynamic overbarrier model, give a fair estimate of the ionization process, these models provide no estimate of the electronic excitation energy that remains in the cluster after the collision and direct ionization [5,14]. In order to get a thorough insight into the nonlinear effects that are likely to play a role in peripheral collisions of highly charged ions with metal clusters, a theoretical model has been recently developed and exploited [5,6,15]; details may be found in Ref. [6] and are summarized here.

In the following sodium clusters are treated within the jellium model, where the ionic background is smeared out uniformly. We will return to that approximation in the next section. For a microscopic description of the interaction between the delocalized electrons and the projectile, we rely on the self-consistent Vlasov equation which provides the time evolution of the electron phase-space distribution function. In our context of use, the Vlasov equation is the semiclassical approximation  $\hbar \rightarrow 0$  of the time-dependent Kohn-Sham (TDKS) equations in the local-density approximation of the time-dependent density-functional theory. This approach allows us to perform calculations over a large range of cluster sizes and projectile parameters. The reliability of this approach was clearly demonstrated in Ref. [15] where TDKS calculations are compared with Vlasov ones. In particular, such observables as the rate of transferred electrons from the

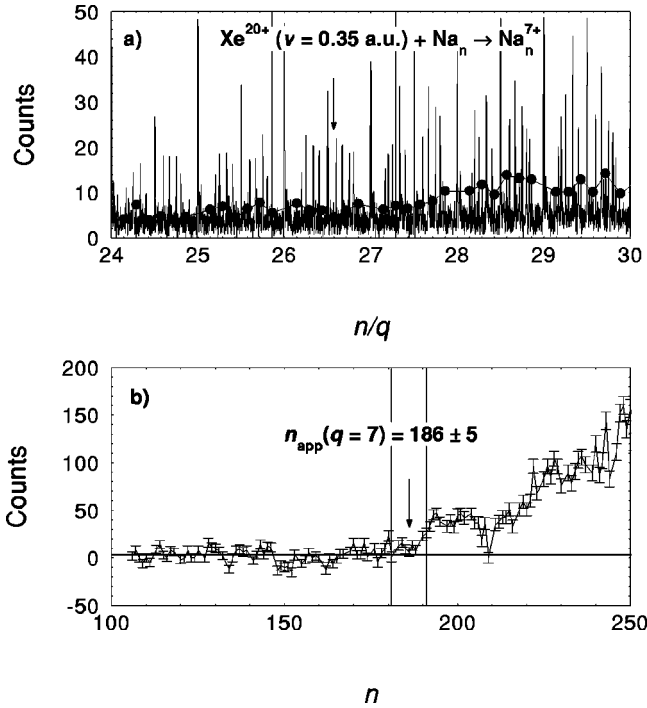


FIG. 2. (a) Time-of-flight mass spectrum of multiply charged sodium clusters  $\text{Na}_n^{q+}$  following the interaction of neutral clusters  $\text{Na}_n$  with  $\text{Xe}^{20+}$  projectiles (kinetic energy  $E=400$  keV, velocity  $v=0.35$  a.u.). The dotted line connects the peaks of sevenfold charged clusters  $\text{Na}_n^{7+}$ . (b) Resulting integral distribution of sevenfold charged clusters  $\text{Na}_n^{7+}$ . The extracted appearance size  $n_{\text{app}}(q=7)$  is indicated on both graphs by an arrow.

cluster to the ion or to the continuum, the final charge and final excitation of the cluster, as well as the electron distribution in the highly excited projectile are in excellent agreement with each other. The calculations discussed in the following have been carried out on the Compaq Alphaserwer SC232 at CEA-Grenoble taking most advantage of parallel techniques [12].

Let us now define the relevant observables for the present discussion. By selecting electrons that at a given time are located inside a sphere of radius twice that of the initial cluster, we construct the residual cluster charge  $q$  after the collision. This charge is well located inside the cluster radius and is stabilized as soon as the projectile leaves the collisional area [5]. The key quantity of present interest is the residual excitation energy  $E^*$  of the ionized  $\text{Na}_n^{q+}$  cluster after a collision. It is defined as  $E^* = E_{\text{final}}(\text{Na}_n^{q+}) - E_{\text{GS}}(\text{Na}_n^{q+})$ , where  $E_{\text{final}}(\text{Na}_n^{q+})$  and  $E_{\text{GS}}(\text{Na}_n^{q+})$  are the final- and ground-state energies of the charged cluster resulting from the collision, respectively. In practice, it is obtained as

$$E^* = E_{\text{final}}(\text{Na}_n^{q+}) - V_{\text{ion}}(0 \rightarrow q, n) - E_{\text{GS}}(\text{Na}_n), \quad (1)$$

where the ionization potential  $V_{\text{ion}}(0 \rightarrow q, n)$  is the energy required to  $q$ -fold ionize the neutral cluster, i.e., the sum of the ionization potentials from 0 to  $q-1$ :

$$V_{\text{ion}}(0 \rightarrow q, n) = E_{\text{GS}}(\text{Na}_n^{q+}) - E_{\text{GS}}(\text{Na}_n). \quad (2)$$

In practice, the excitation energies have been worked out as follows. As the projectile approaches the cluster, it distorts considerably the electron cloud until electrons jump from the cluster to the multiply charged ion. As the collision proceeds further, a flow of electronic fluid develops between the target and the projectile. The nonlinear dynamics is followed over a length of time of about 50 fs, much larger than the interaction time of the order of a few fs. At that time, one evaluates the residual charge  $q$  of the ionized cluster as well as its total energy  $E^*$ . This allows us to calculate the excitation energy from Eq. (1), the ionization potentials being first obtained as described below.

Ground-state energies have been calculated for the set of cluster sizes  $n=40, 58, 92, 138, 196, 256$  and  $334$ , and charges  $q=1, 2, 4$ , and  $10$ . This covers the range of experimentally attainable values. Then, the resulting ionization potentials have been fitted by a quadratic law such as

$$V_{\text{ion}}(0 \rightarrow q, n) = a(n)q + b(n)q^2. \quad (3)$$

Such a dependence of the total ionization potential is expected for conducting spheres and has been confirmed by photoionization experiments on neutral clusters [11,16]; the ionization potential (in atomic units) of a cluster with charge  $q$  and size  $n$  is given by

$$V_{\text{ion}}(q, n) = W_b + \left( \frac{\alpha + q}{r_{\text{ws}}} \right) n^{-1/3}, \quad (4)$$

where  $W_b$  is the bulk work function of sodium,  $r_{\text{ws}}$  is the Wigner-Seitz radius, and  $\alpha$  is a constant. For sodium,  $W_b \approx 0.1$  a.u.,  $r_{\text{ws}} \approx 4.0$  a.u., and  $\alpha \approx 0.4$  [16,11]. From Eq. (4), one easily derives the quadratic dependence

$$V_{\text{ion}}(0 \rightarrow q, n) = \sum_{k=1}^{q-1} V_{\text{ion}}(k, n) = \left[ W_b + \left( \alpha - \frac{1}{2} \right) \frac{1}{r_{\text{ws}}} n^{-1/3} \right] q + \left( \frac{1}{2r_{\text{ws}}} n^{-1/3} \right) q^2. \quad (5)$$

As shown in Table I, the fitted values of the parameters  $a(n)$  and  $b(n)$  are in good agreement with Eq. (5) assuming bulk values for the parameters  $W_b$  and  $r_{\text{ws}}$  [16]. Ionization potential curves are displayed in Fig. 3.

#### IV. RESULTS AND DISCUSSION

During a peripheral collision, the electric field associated with the projectile charge  $z$  appears to the cluster as a single broad pulse, whose width is about 10 fs for the projectile velocities used, and whose magnitude remains below 0.1 a.u. On this time scale, the conduction electrons cloud follows quasiadiabatically the variations of the electric field whereas the ions remain inert. This justifies the use of the jellium model as to the qualitative evolution of the final charge and excitation energy as a function of the collision parameters. Indeed, our calculations, either quantal or semi-classical [15], indicate that in such peripheral collisions the

TABLE I. Fitted values of  $a(n)$  and  $b(n)$  as obtained with the semiclassical Vlasov equation (left part) and the classical electrostatic formula Eq. (5) (right part) for cluster sizes  $N=40, 58, 92, 138, 196, 256$ , and  $334$ .

$N$	$a(N)$	$b(N)$	$a^{(cl)}(N)$	$b^{(cl)}(N)$
40	2.253	1.002	2.5015	0.9942
58	2.5026	0.8612	2.5304	0.8784
92	2.4396	0.7477	2.5617	0.7532
138	2.5522	0.6389	2.5855	0.6579
196	2.8340	0.5714	2.6037	0.5853
256	2.6094	0.5228	2.6161	0.5355
334	2.5837	0.4832	2.6275	0.4900

cluster ionization arises mainly from a direct transfer of conduction electrons to the projectile ion. Once the outgoing excited atom leaves the interaction zone, the residual cluster charge remains perfectly stable and the cluster is in some excited state. As discussed in Refs. [12,17], this is in net contrast with the interaction with a femtosecond laser pulse characterized by a fast oscillation (period around 1 fs) of an electric field with the same order of magnitude. In these works, we have studied the coupled dynamics of delocalized electrons and ions in sodium clusters under irradiation by a strong femtosecond laser pulse, the electrons being described with the semiclassical equation and ions being treated classically. A comparison between a laser experiment and a collision that yields the same final charge on the same time scale reveals a very large difference in the amount of residual electronic excitation as well as in the kinetic energy transferred to the ions. The heating of the ions is much slower in the collision simulation than in the laser one. This is due to the rapid electronic oscillations in the laser field across the ionic background that heat the electron cloud much more than does a passing projectile, which draws globally the electronic cloud towards it. The laser-induced “hot electrons” boost the kinetic ionic energy strongly, which results in a

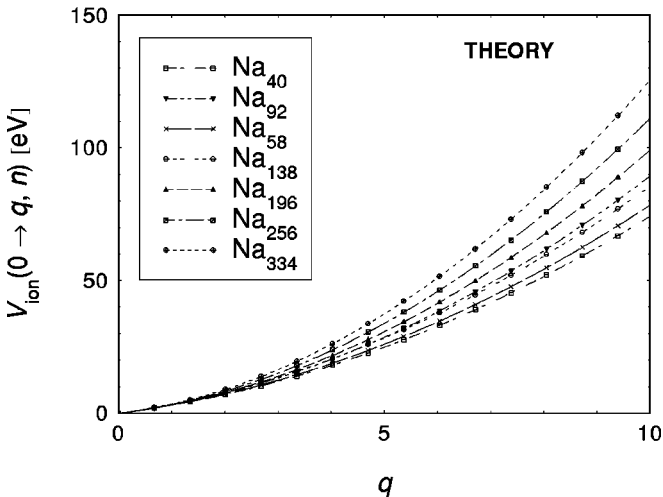


FIG. 3. Ionization potential  $V_{\text{ion}}(0 \rightarrow q, n)$  of sodium clusters for sizes  $N=40, 58, 92, 138, 196, 256$ , and  $334$  as obtained by evaluating the semiclassical ground-state energies in Eq. (2).

faster cluster dissociation due to the combined effect of the Coulomb forces and of the electronic kinetic pressure.

The use of the jellium model would no longer be appropriate if we were also interested in the relaxation of the excitation energy after the collision because the discrete ionic structure has a noticeable influence on the relaxation mechanisms [12,18]. Here in order to compare the theoretical results, which yield the residual charge and excitation energy of the cluster after the collision with the projectile ion, to the experimental appearance sizes, measured about  $100 \mu\text{s}$  after the collisional process, we can safely assume that the whole of the final excitation energy is converted into an ionic temperature. This process should take a few ps, as shown by recent pump-probe experiments [19]. The increase of temperature will add to the genuine Coulomb instability a thermal instability resulting in appearance sizes  $n_{\text{app}}(q)$  above the Rayleigh critical size  $n_{\text{crit}}(q)$  ( $T=0$  K) [11].

As we will see in the following, both experimental and theoretical data show a nontrivial evolution of the residual excitation energy on the following parameters: the projectile charge  $z$  and velocity  $v$ , the impact parameter  $b$ , and the cluster size  $n$ . In an experiment,  $z$  and  $v$  can be selected but the measurements average over all impact parameters  $b$ . The experimental observable, the appearance size  $n_{\text{app}}(q)$ , is a probe of the excitation energy  $E^*[n, z, b, v]$  transferred to the cluster in the collision close to that size. Clusters  $\text{Na}_n^{q+}$  with  $n$  close to  $n_{\text{app}}(q)$  do not undergo any activated process between the collision and the detection and their charge  $q$  and size  $n$  are those prevailing just after the collision. This was indeed confirmed by simulations of time-of-flight spectra taking into account the different thermally activated processes (fission, evaporation) [20]. But this is no longer true when further deviating from  $n_{\text{app}}(q)$  where the distribution of clusters  $\text{Na}_n^{q+}$  of charge  $q$  has contributions of clusters with higher charges  $q+1, q+2, \dots$  due to sequential fission and/or evaporation events. In the following, we will therefore compare  $n_{\text{app}}(q)$  (experiment) with  $E^*[n, z, b, v]$  (theory) (this quantity will be denoted by  $E^*$ ). Apart from expected qualitative behavior, the global variation of  $E^*$  is not easily foreseeable because of the importance of the dynamical effects.

*Influence of the projectile charge  $z$ .* In our previous work [9], we measured and discussed the appearance size of multiply charged sodium clusters  $\text{Na}_n^{q+}$  ( $q \leq 10$ ) formed in collisions of neutral clusters with low-energy multiply charged ions  $A^{z+}$  ( $z \leq 28, v \approx 0.4$  a.u.):  $n_{\text{app}}(q)$  decreases strongly when increasing the projectile charge  $z$  and converges towards an asymptotic limit where the fissility  $X$  equals about 0.8, close to the Rayleigh limit ( $X=1$ ). This is illustrated on Fig. 4 for two distinct projectile charges  $z=8$  and  $z=25$  at the same velocity  $v \approx 0.4$  a.u.: the larger the projectile charge is, the lower the appearance size is. This behavior is explained by the difference in the residual excitation energy of the ionized clusters after the collision. We show in Fig. 5 how the electronic excitation  $E^*$  depends upon its net residual charge  $q$  for the set of cluster sizes  $n=58, 138, 256$ , and  $334$  and two distinct projectile charge  $z=8$  and  $z=25$  with  $v=0.4$  a.u., each point corresponding to a calculation

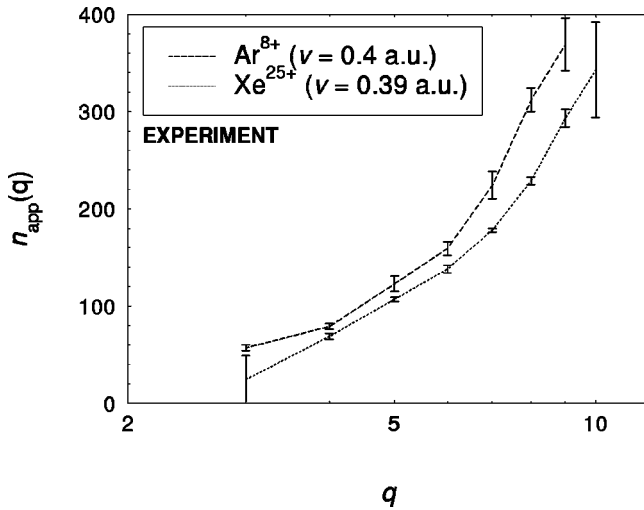


FIG. 4. Experimental appearance size  $n_{app}(q)$  as a function of the cluster final charge  $q$  for projectile ions  $Ar^{8+}$  ( $E = 160$  keV,  $v = 0.4$  a.u.) and  $Xe^{25+}$  ( $E = 500$  keV,  $v = 0.39$  a.u.).

at a given impact parameter  $b$ . In each case, the excitation energy for a given  $q$  depends strongly on the initial projectile charge  $z$ . Our data confirm that, when  $z$  increases, collisions occur at larger impact parameters where excitation is less probable. Correspondingly the internal energy of the ionized

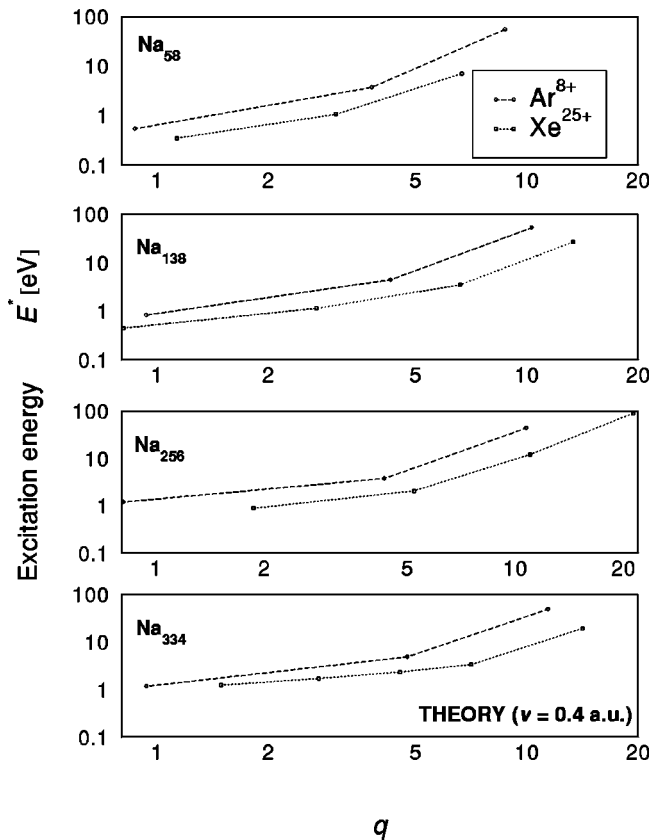


FIG. 5. Theoretical excitation energy  $E^*$  as a function of the cluster final charge  $q$  for projectile ions  $Ar^{8+}$  and  $Xe^{25+}$  with the same velocity  $v = 0.4$  a.u. for the cluster sizes  $n = 58, 138, 256,$  and  $334$ .

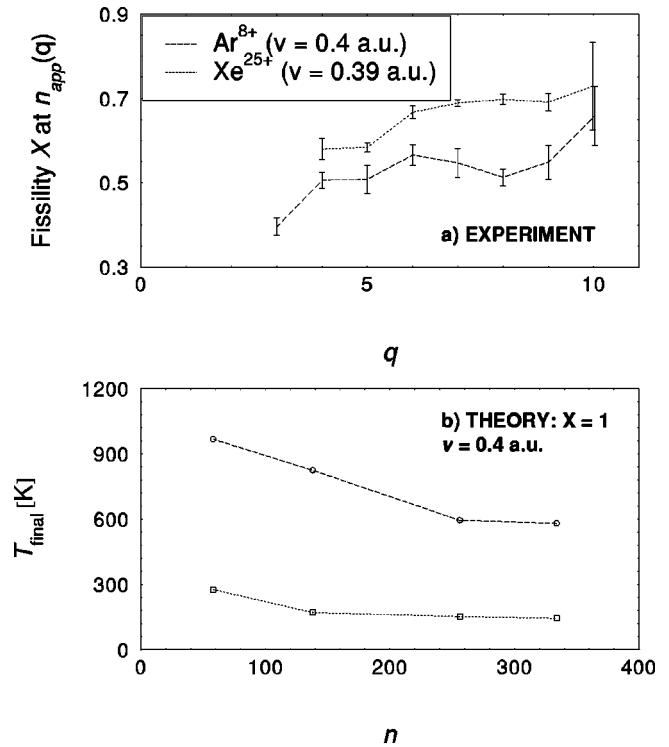


FIG. 6. (a) Experimental fissilities corresponding to the appearance sizes  $n_{app}(q)$  of Fig. 4 measured for the projectile ions  $Ar^{8+}$  ( $E = 160$  keV,  $v = 0.4$  a.u.) and  $Xe^{25+}$  ( $E = 500$  keV,  $v = 0.39$  a.u.). (b) Theoretical cluster final temperature at the critical charge ( $X = 1$ ) for the projectile ions  $Ar^{8+}$  and  $Xe^{25+}$  at  $v = 0.4$  a.u.

system is lower and cannot activate the fission process. Therefore, high projectile charges (typically above 20) should be used in order to minimize the residual excitation energy of the cluster ions  $Na_n^{q+}$ .

*Influence of the cluster size  $n$ .* The dependence of the previous results on the cluster size is also very instructive. We show in Fig. 6(a) the experimental fissilities measured at the appearance size  $n_{app}(q)$  for the data set of Fig. 4. One can see that for both projectile charges  $z$ , the highest fissility is obtained for the highest final cluster charge  $q$ . This effect is counterintuitive as one would expect that the larger  $q$  is, the smaller the impact parameter  $b$  is and, therefore, the larger  $E^*$  is, resulting in higher appearance sizes  $n_{app}(q)$  [5,6]. But as the appearance  $n_{app}(q)$  roughly scales with  $q^2$ , those with the highest  $q$  also possess the largest number of internal degrees of freedom (this quantity roughly scales as  $3n$ ). They can accumulate more internal energy without decaying and therefore approach closer the Rayleigh limit, as observed in Fig. 6(a).

Our calculations reproduce well this effect. By interpolating the excitation energies of Fig. 5 by a power law ( $E^* = aq^c + b$ ), one can evaluate the residual excitation of clusters  $Na_n^{q_{crit}}$ , where  $q_{crit}$  is the critical Rayleigh charge for each cluster size  $n = 58, 138, 256,$  and  $334$ . The calculated energy is then converted into an ionic temperature  $T_{final}$  which adds to the initial neutral cluster temperature. The results are displayed in Fig. 6(b) for the cluster sizes  $n = 58, 138, 256,$  and  $334$ . For both projectile charges  $z = 8$  and  $25$ ,  $T_{final}$  decreases

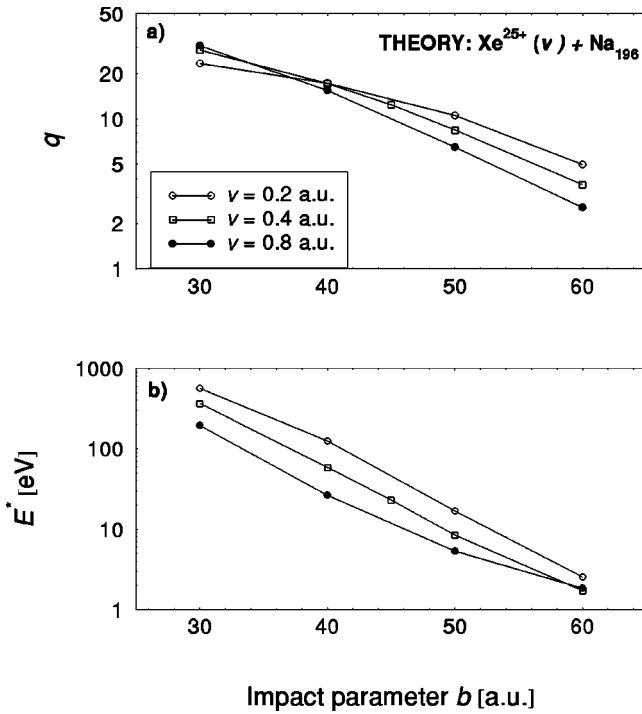


FIG. 7. Evolution of the final charge and of the final excitation energy as a function of the impact parameter and projectile velocity for the collision system  $\text{Xe}^{25+} + \text{Na}_{196}$  at  $v = 0.2, 0.4$ , and  $v = 0.8$  a.u.

when  $n$  increases, in agreement with experiment. The evolution of the fissility at the appearance size with  $q$  for a given projectile is therefore due to a balance between  $E^*$  and the number of degrees of freedom which yields colder clusters for higher  $q$ . Ultimately, the fissility converges towards an asymptotic value which depends on the initial cluster tem-

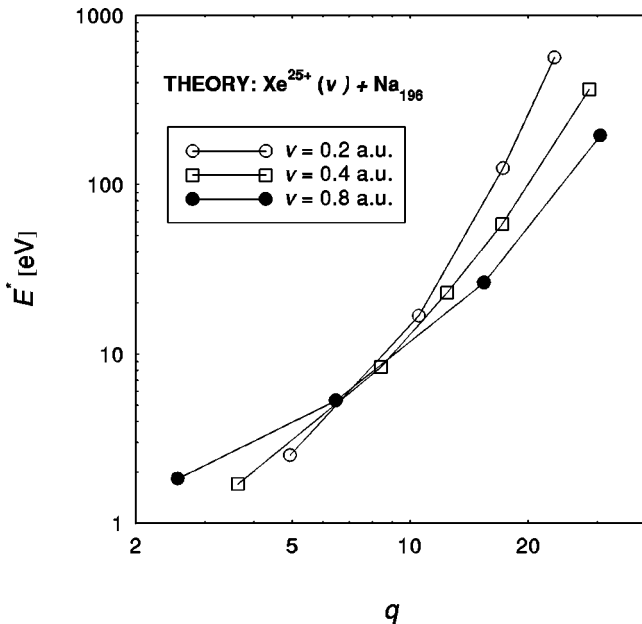


FIG. 8. Residual electronic excitation energy as a function of the net final charge for the same data set as in Fig. 8.

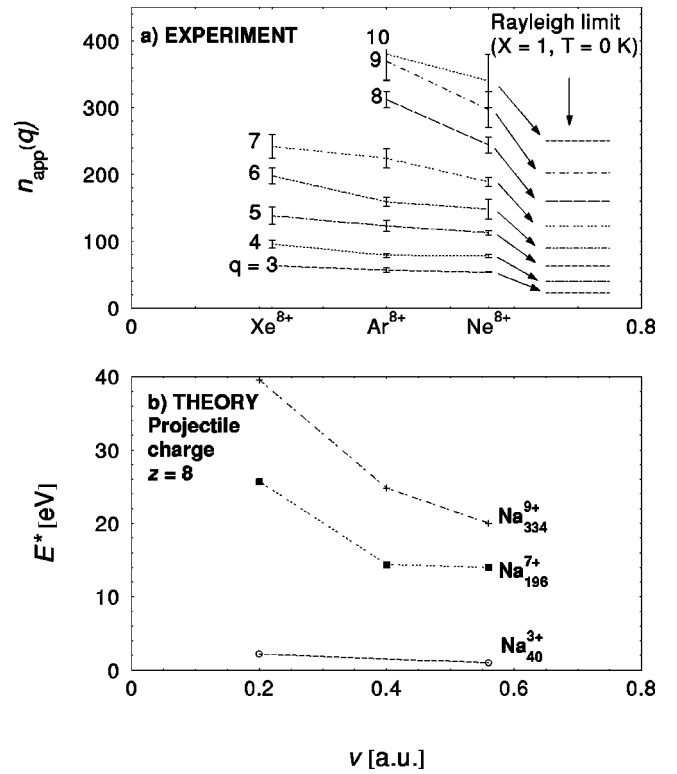


FIG. 9. (a) Appearance size  $n_{\text{app}}(q)$  of  $q$ -fold charged clusters  $\text{Na}_n^{q+}$  as a function of the projectile velocity for the projectile charge  $z = 8$ . On the right side the Rayleigh limit is indicated. (b) Excitation energy  $E^*$  of clusters at the critical charge ( $n = 2.5q^2$ ) as a function of the projectile velocity for  $z = 8$ .

perature. This limit also gets closer to  $X = 1$  as the cluster charge and/or size increase, as discussed in our previous work in the framework of the Bohr and Wheeler model for the fission barrier height [9]. In conclusion, to further approach the Rayleigh limit requires us to use not only high projectile charges  $z$  but also to consider larger cluster sizes.

*Influence of the projectile velocity.* Due to dynamical effects, the residual cluster excitation depends on the relative velocity of the projectile compared to the Fermi velocity of the conduction electrons (around 0.35 a.u. for sodium). In Fig. 7 we have plotted the final cluster charge  $q$  (a) and excitation energy  $E^*$  (b) as a function of the impact parameter  $b$  for the collision system  $\text{Na}_{196}$  ( $R \approx 23$  a.u.) +  $\text{Xe}^{25+}$  at different projectile velocities  $v = 0.2, 0.4$  and  $v = 0.8$  a.u. For truly peripheral collisions, i.e., far more than twice the cluster radius, the Vlasov calculation predicts a decrease of the ionization rate when increasing the velocity. This trend is reversed for closer collisions. As to the excitation energies, there is a crossing point in the regimes as can be seen in Fig. 8. For the smallest final charges, larger projectile velocities lead to lower final excitation energies and the opposite is observed for  $q \geq 10$ . This latter case corresponds to collisions with lower impact parameters. Similar trends are obtained with other projectile charges but with different crossing points.

Experimentally, we are in the high-charge regime as illustrated in Fig. 9. The upper part of the graph shows the evolution of  $n_{\text{app}}(q)$  for projectile ions with  $z = 8$  of various

velocities. Experimentally, we used different ions of charge 8 ( $\text{Xe}^{8+}$ ,  $\text{Ar}^{8+}$ , and  $\text{Ne}^{8+}$ ) with the same kinetic energy  $E = 160$  keV at which the ion accelerator performances are optimal. Changing the core ion without changing the projectile charge should not affect the final charge state of the cluster, especially for peripheral collisions. The higher the ion velocity, the lower the appearance size  $n_{\text{app}}(q)$ . The effect is more pronounced for the highest cluster charges  $q$ . In the lower part of Fig. 9, we have plotted the theoretical excitation energy  $E^*$  for the same projectile charge  $z=8$  as a function of velocity  $v$  for cluster charges  $q=3, 7$ , and  $9$  with sizes close to the experimental appearance sizes for the same charges. The faster the projectile, the lower the excitation energy in agreement with the experimental results. It then turns out that to generate colder multiply charged clusters  $\text{Na}_n^{q+}$ , it is appropriate to use projectile velocities close to or higher than the Fermi velocity.

## V. SUMMARY

In conclusion, we have studied experimentally and theoretically the influence of the collision parameters on the excitation energy  $E^*$  transferred in low-energy ion-metal cluster collisions and their influence on the appearance size  $n_{\text{app}}(q)$ . To study the onset of charge instabilities in low excited systems, it turns out that the best choice is to use high projectile charges ( $z \geq 25$ ) with velocities above  $0.5$  a.u. and large clusters for which the high number of internal degrees of freedom allow us to minimize the effect of  $E^*$ . An alternative but experimentally more demanding route is to use colder sodium clusters targets, e.g., by cooling the cluster source with liquid helium.

On the basis of the above discussion, it is interesting to extrapolate the experimental results discussed above at much larger cluster sizes. On the experimental time scale, the mini-

mum barrier height that clusters  $\text{Na}_n^{q+}$  thermalized at  $100$  K can survive is  $B_{\text{fission}} \approx 0.18$  eV [9]. This can be related to a fissility by the Bohr-Wheeler formula for the fission barrier height, valid for fissilities close to 1,

$$B_{\text{fission}}(\text{Na}_n^{q+}) = \frac{98}{135} E_s (1-X)^3 \propto n^{2/3} (1-X)^3, \quad (6)$$

where  $E_s = a_s n^{2/3}$  is the surface energy and  $a_s$  is the surface tension (between  $0.7$  and  $1$  eV for sodium, depending on the temperature [11]). Using the parameters for sodium and reverting the formula gives the relationship between size and fissility for a given barrier height. For  $B_{\text{fission}} \approx 0.18$  eV, we get  $n \approx 0.2/(1-X)^{9/2}$ . For  $X=0.85$ , the maximum fissility experimentally observed, this gives  $n \approx 1000$ , i.e., in the cluster size range studied here. For  $X=0.99$ , this gives  $n \approx 2 \times 10^8$ , corresponding to a cluster radius  $R = r_{\text{ws}} \times n^{1/3} \approx 2400$  a.u.  $\approx 0.130$   $\mu\text{m}$ , i.e., in the micrometric size range ( $r_{\text{ws}} \approx 4$  a.u. is the Wigner-Seitz radius of sodium [11]). Indeed, fissilities close to the Rayleigh limit were measured in recent experiments on micrometric ethylene glycol droplets, consistently with our extrapolated results on nanometric metallic clusters [21].

## ACKNOWLEDGMENTS

The experiments presented in this work were performed at the Accélérateur d'Ions Multichargés (AIM) at CEA-Grenoble. Stimulating discussions with C. Ristori during the designing stage of the experiment are gratefully acknowledged. We would like to thank D. Cormier and F. Gustavo for the preparation of the ion beams and H. Lebius for his participation in some of the experiments. We acknowledge the important contribution of L. Plagne who wrote the first version of the theoretical code used in this work.

- 
- [1] H. Cederquist *et al.*, Phys. Scr. **T80**, 46 (1999).  
 [2] B. Walch *et al.*, Phys. Rev. Lett. **72**, 1439 (1994).  
 [3] F. Chandezon *et al.*, Phys. Rev. Lett. **74**, 3784 (1995).  
 [4] S. Martin *et al.*, Phys. Rev. A **59**, R1734 (1999); Eur. Phys. J. D **12**, 27 (2000).  
 [5] L. Plagne and C. Guet, Phys. Rev. A **59**, 4461 (1999).  
 [6] L. Plagne, Ph.D. thesis, Université Joseph Fourier, Grenoble, 1999.  
 [7] P.-G. Reinhard, E. Suraud, and C.A. Ullrich, Eur. Phys. J. D **1**, 303 (1998).  
 [8] C. Guet *et al.*, Z. Phys. D: At., Mol. Clusters **40**, 317 (1997); T. Bergen *et al.*, in *Similarities and Differences Between Atomic Nuclei and Clusters, Tsukuba 1997*, edited by Y. Abe *et al.*, AIP Conf. Proc. No. 416 (AIP, Woodbury, NY, 1997), p. 148.  
 [9] F. Chandezon *et al.*, Phys. Rev. Lett. **87**, 153402 (2001).  
 [10] Lord Rayleigh, Philos. Mag. **14**, 185 (1882).  
 [11] U. Näher *et al.*, Phys. Rep. **285**, 245 (1997).  
 [12] J. Daligault, Ph.D. thesis, Université Joseph Fourier, Grenoble, 2001.  
 [13] T. Bergen *et al.*, Rev. Sci. Instrum. **70**, 3244 (1999).  
 [14] J. Burgdörfer, P. Lerner, and F.W. Meyer, Phys. Rev. A **44**, 5674 (1991).  
 [15] L. Plagne *et al.*, Phys. Rev. A **61**, 033201 (2000).  
 [16] W.A. de Heer, Rev. Mod. Phys. **65**, 611 (1993).  
 [17] J. Daligault and C. Guet, Phys. Rev. A **64**, 043203 (2001).  
 [18] J. Daligault and C. Guet (unpublished).  
 [19] J.-Y. Bigot, V. Halté, J.-C. Merle, and A. Daunois, Chem. Phys. **251**, 181 (2000).  
 [20] G.E. N'tamack *et al.*, J. Phys. B **35**, 2729 (2002).  
 [21] D. Duft *et al.*, Phys. Rev. Lett. **89**, 084503 (2002).